Lecture 7. Types of inverse problems, model reduction, model identification.

Part B. Modal reduction for thermal problems: Core principles and presentation of theAROMM method

F. Joly, **Y. Rouizi**, **O. Quéméner**

Laboratoire de Mécanique et d'Energétique d'Evry, Univ. Paris-Saclay
40 rue du Pelvoux, Courcouronnes 91020 Evry, France

E-mail: f.joly@iut.univ-evry.fr
yassine.rouizi@univ-evry.fr
o.quemener@iut.univ-evry.fr

Abstract. In the second part of this lecture, the special case of modal reduction is discussed. This method allows to greatly reduce the size of the model in case of complex geometry. The principle of this technique is presented. A focus on the AROMM method is carried out. We insist on the necessity to choose a modal basis adapted to the physical problem. Different principles of reduction are introduced.

Scope

1 Introduction

As computer hardware is developing, the requirements for numerical simulation are becoming more demanding.
First, geometries have to perfectly match the reality of the simulated object. A recent study [1] has shown that the exact numerical modeling of a simple electronic component needs a mesh of $422k$ nodes. This order of magnitude has to be compared to industrial demand, that is to obtain the simulation of an entire electronic card.
Furthermore, we are also demanding for more and more realistic consideration of physical phenomena. In thermal problems, infrared radiations for example, highly complicates the heat transfer simulations [2].
Considering the inverse approach, this effect is amplified by the iterative procedure which involves the use of an important number of simulations [1].
For all those reasons, model reduction is a topical issue. The idea consists in searching the whole temperature field by using a small number of unknowns.

2 Context of the study: the heat equation

The problem is the following: the domain Ω, delimited by boundary Γ, is characterized by its thermal conductivity $k(M,t)$ [W.m^{-1}.K^{-1}] and its volumetric heat capacity $c(M,t)$ [J.m^{-3}.K^{-1}]. This domain receives two types of thermal loadings:

- the influence of the environment, which is characterised by a temperature $T_f(M,t)$ $[K]$ and a heat exchange coefficient $h(M,t)$ [W.m^{-2}.K^{-1}],
- the thermal dissipation, which can be a volumetric power on the domain $\pi(M,t)$ [W.m^{-3}] or a surface load on the border $\varphi(M,t)$ [W.m^{-2}].

Such a problem is modeled by the following equations:

$$\left\{ \begin{array}{lll} \forall M \in \Omega & : & c\dfrac{\partial T}{\partial t} = \overrightarrow{\nabla} \cdot (k \overrightarrow{\nabla} T) + \pi \\ \forall M \in \Gamma & : & k \overrightarrow{\nabla} T \cdot \overrightarrow{n} = \varphi + h(T_f - T) \end{array} \right. \tag{1}$$

For complex geometries, the solution of this problem is numerical and needs a spatial discretization. Let g be the test function, defined on the Hilbert space $H^1(\Omega)$. The weak variational formulation of Eq. (1) writes:

$$\begin{array}{rl} \forall g \in H^1(\Omega), \quad \displaystyle\int_\Omega g\, c\, \frac{\partial T}{\partial t}\, d\Omega = & -\displaystyle\int_\Omega k \overrightarrow{\nabla} g \cdot \overrightarrow{\nabla} T \, d\Omega - \int_\Gamma g\, h\, T \, d\Gamma \\ & + \displaystyle\int_\Omega g\, \pi \, d\Omega + \int_\Gamma g\, (\varphi + h\, T_f)\, d\Gamma \end{array} \tag{2}$$

It should be noted that it would be possible to consider:

- an anisotropic thermal conductivity characterized by a tensor $\overline{\overline{\mathbf{k}}}$,
- an advection - conduction problem, by adding a transport term to the heat equation,
- infrared radiation between boundaries.

[1] In case of linear inverse problem, even if it is possible to use a direct procedure, this one needs one matrix inversion.

The addition of these terms does not change anything for the reduction method, and we will consider afterwards the problem defined by Eq. (1).
The spatial discretization of Eq. (2) leads to the following equation (according to the order of terms) :

$$\mathbf{C}\frac{d\mathbf{T}}{dt} = \mathbf{A}\mathbf{T} + \mathbf{U} \tag{3}$$

where $\mathbf{C}$ et $\mathbf{A}$ are respectively the capacity and the conductivity matrices, of dimension $[N \times N]$, where N is the number of degrees of freedom (DOF) for the considered discretized domain. $\mathbf{T}$ is the temperature vector, which depends on time, and $\mathbf{U}$ is the load vector. The dimension of all these vectors are $[N]$.
This equation constitutes the complete heat problem, and might be characterized by a large number of DOF[2] in case of complex geometry.

3 The modal reduced model principle

This method is based on time-space separation:

$$T(M,t) = \sum_{i=1}^{\infty} V_i(M)\, x_i(t) \tag{4}$$

Considering the space functions $V_i(M)$ as being known, the determination of the temperature field results in computing excitation states $x_i(t)$. It is important to notice that relation (4) is true only if the set of spatial functions $V_i(M)$ form a basis of the solutions space of the thermal problem (2), which is not always garanted.
The idea is then to rewrite this formulation using a limited number n of space functions $\widetilde{V}_i(M)$, that leads to an acceptable reconstitution of the thermal fields $\widetilde{T}(M,t) \simeq T(M,t)$:

$$\widetilde{T}(M,t) = \sum_{i=1}^{n} \widetilde{V}_i(M)\, \widetilde{x}_i(t) \tag{5}$$

Whatever the reduction technique used, the reduced model is obtained by projection of the heat equation on the subspace defined by the space functions $\widetilde{V}_i(M)$. Equation (2) becomes:

$$\begin{aligned} &\forall g \in H^1(\Omega), \\ &\int_\Omega g\, c\, \frac{\partial}{\partial t}\left(\sum_{i=1}^{n} \widetilde{V}_i\, \widetilde{x}_i\right) d\Omega = \\ &\qquad -\int_\Omega k \overrightarrow{\nabla} g \cdot \overrightarrow{\nabla}\left(\sum_{i=1}^{n} \widetilde{V}_i\, \widetilde{x}_i\right) d\Omega - \int_\Gamma g\, h \left(\sum_{i=1}^{n} \widetilde{V}_i\, \widetilde{x}_i\right) d\Gamma \\ &\qquad + \int_\Omega g\, \pi\, d\Omega + \int_\Gamma g\, (\varphi + hT_f)\, d\Gamma \end{aligned} \tag{6}$$

Considering that the set of spatial functions $\widetilde{V}_i(M)$ forms an approximated basis for the physical problem, these functions can be used as test functions for the variational formulation: $g(M) = \widetilde{V}_j(M)$. After rearrangement, we have:

[2] For a finite differences method or for a finite elements method for which the interpolation functions are linear, the DOF corresponds to the mesh nodes.

$$
\begin{aligned}
&\forall\ \widetilde{V}_j \in H^1(\Omega), j \in \{1,n\},\\
&\quad \sum_{i=1}^{n} \left(\int_\Omega \widetilde{V}_j\ c\ \widetilde{V}_i\, d\Omega \right)\ \frac{d\widetilde{x}_i}{dt} =\\
&\qquad -\sum_{i=1}^{n} \left(\int_\Omega k \overrightarrow{\nabla}\widetilde{V}_j \cdot \overrightarrow{\nabla}\widetilde{V}_i\, d\Omega + \int_\Gamma \widetilde{V}_j\, h\, \widetilde{V}_i\, d\Gamma \right)\ \widetilde{x}_i\\
&\qquad + \int_\Omega \widetilde{V}_j\, \pi\, d\Omega\ + \int_\Gamma \widetilde{V}_j\, (\varphi + hT_f)\, d\Gamma
\end{aligned}
\tag{7}
$$

After spatial discretization, function $\widetilde{V}_i(M)$ becomes a vector $\widetilde{\mathbf{V}}_i\,[N]$ resulting in:

$$
\forall\ j \in \{1,n\}\,, \quad \sum_{i=1}^{n} \widetilde{\mathbf{V}}_j^{\ t}\ \mathbf{C}\ \widetilde{\mathbf{V}}_i\ \ \frac{d\widetilde{x}_i}{dt} = -\sum_{i=1}^{n} \widetilde{\mathbf{V}}_j^{\ t}\ \mathbf{A}\widetilde{\mathbf{V}}_i\ \widetilde{x}_i + \widetilde{\mathbf{V}}_j^{\ t}\ \mathbf{U} \tag{8}
$$

We name $\widetilde{\mathbf{V}}\,[N \times n]$ the matrix which gathers the n discretized functions $\widetilde{\mathbf{V}}_i\,[N]$, and $\widetilde{\mathbf{X}}(t)\,[n]$ the vector of the n time-dependent excitation states $\widetilde{x}_i(t)$ associated to the space functions:

$$
\widetilde{\mathbf{V}}^{\ t}\ \mathbf{C}\ \widetilde{\mathbf{V}}\ \frac{d\widetilde{\mathbf{X}}}{dt} = \widetilde{\mathbf{V}}^{\ t}\ \mathbf{A}\ \widetilde{\mathbf{V}}\ \widetilde{\mathbf{X}} + \widetilde{\mathbf{V}}^{\ t}\ \mathbf{U} \tag{9}
$$

Under compact form:

$$
\mathbf{L}\ \frac{d\widetilde{\mathbf{X}}}{dt} = \mathbf{M}\ \widetilde{\mathbf{X}} + \mathbf{N} \tag{10}
$$

with $\mathbf{L} = \widetilde{\mathbf{V}}^{\ t}\ \mathbf{C}\ \widetilde{\mathbf{V}}$ and $\mathbf{M} = \widetilde{\mathbf{V}}^{\ t}\ \mathbf{A}\ \widetilde{\mathbf{V}}$ whose dimensions are $[n \times n]$, and vector $\mathbf{N} = \widetilde{\mathbf{V}}^{\ t}\ \mathbf{U}\ [n]$.

This formulation leads to the reduction of the number of DOF, because the complete model given by Eq. (3) is characterized by N unknowns, while the dimension of the modal model defined by Eq. (10) corresponds to the n space functions $\widetilde{V}_i(M)$.

From this formulation, different methods exist to retrieve the modes:

- The principle of the POD (*Proper Orthogonal Decomposition*) is the identification of the space functions $\widetilde{V}_i(M)$ from several reference temperature fields (noted $T_{ref}(M,t)$ for a thermal problem). This technique has been used in a lot of studies [3, 4, 5, 6, 7, 8, 9, 10].
- The MIM (*Modal Identification Method*) is based on the direct identification of the matrices of Eq. (10) from simulations or measurements. This technique has been widely used for inverse problems [11, 12, 13, 14, 11, 15, 16].
- The PGD (*Proper Generalized decomposition*) is a generalization of the decomposition principle: the temperature is written as a multiple product of a set of functions, where each of these functions depends on one variable (time, space) or on one parameter (heat capacity, thermal conductivity, ...). These functions are computed by enriching the basis at each iteration [17, 18, 19, 20].

- The AROMM (Amalgam Reduced Order Modal Model) method follows both steps which appear in the modal principle, that is:
  - to compute a complete basis $\{V_i(M)\}_{i\in\mathbb{N}}$, on which it is possible to proceed to a rigorous decomposition of the thermal fields:

$$T(M,t) = \sum_{i=1}^{\infty} V_i(M)\, x_i(t) \tag{11}$$

  - to obtain a reduced basis $\{\tilde{V}_i(M)\}_{i\in[1,n]}$, in order to decrease the model order[3] while keeping a satisfactory estimation of the thermal field:

$$T(M,t) \simeq \sum_{i=1}^{n} \widetilde{V}_i(M)\, \widetilde{x}_i(t) \tag{12}$$

The goal of this lecture consists in presenting this method.

4 The complete basis computation

We search a set of spatial functions that forms a basis for the considered thermal problem. This set depends on the solutions space.

4.1 Classical basis

4.1.1 The Fourier basis

We first consider a thermal problem characterized by homogeneous boundary conditions:

$$\begin{cases} \forall M \in \Omega \quad : \quad c_0 \dfrac{\partial T}{\partial t} = \overrightarrow{\nabla} \cdot (k_0 \overrightarrow{\nabla} T) + \pi \\ \forall M \in \Gamma \quad : \quad k_0 \overrightarrow{\nabla} T \cdot \overrightarrow{n} = -h_0\, T \end{cases} \tag{13}$$

The physical parameters (heat capacity c_0, thermal conductivity k_0, and global heat exchange coefficient h_0) are functions of space only.
Functions $\hat{V}_i^F(M)$ are solutions of the eigenvalue problem associated to the physical problem:

$$\begin{cases} \forall M \in \Omega \quad : \quad \overrightarrow{\nabla} \cdot \left(k_0 \overrightarrow{\nabla} \hat{V}_i^F \right) = z_i^F\, c_0\, \hat{V}_i^F \\ \forall M \in \Gamma \quad : \quad k_0 \overrightarrow{\nabla} \hat{V}_i \cdot \overrightarrow{n} = -h_0\, \hat{V}_F \end{cases} \tag{14}$$

z_i^F [s^{-1}] is the eigenvalue associated to each eigenvector $\hat{V}_i^F$. The inverse of this quantity is a time τ_i^F [s] named the time constant of the eigenvector. It characterizes the dynamic of the eigenmode:

$$\tau_i^F = \frac{-1}{z_i^F} \tag{15}$$

Fourier eigenmodes (Figure 1.a) can be considered as particular temperature fields: the eigenvalue problem corresponds to a stationary physical problem with a volumetric thermal load proportional to the eigenmode value at each point of the domain, and with homogeneous boundary conditions.

[3] As we will see later, the reduced functions $\tilde{V}_i(M)$ do not correspond necessary to the functions $V_i(M)$ of the complete basis. This explains the change of notation

The variational formulation of the eigenvalue problem reads :

$$\forall g \in H^1(\Omega), \quad -\int_\Omega k_0 \overrightarrow{\nabla} g \cdot \overrightarrow{\nabla} \hat{V}_j^F \, \partial\Omega - \int_\Gamma g \, h_0 \, \hat{V}_i^F = z_i^F \int_\Omega g \, c_0 \, \hat{V}_i^F \, \partial\Omega \tag{16}$$

For complex geometries, such eigenvalue problem is solved numerically, from a spatial discretization characterized by N DOF. The number of numerically accessible eigenmodes becomes finite and equal to N. The numerical solution is performed by the Lanczos method [21], from the discrete formulation of Eq. (16). Using the same matrix than specified previously (Eq. (3)), we have:

$$\mathbf{A} \ \hat{\mathbf{V}}_i^F = z_i^F \ \mathbf{C} \ \hat{\mathbf{V}}_i^F \tag{17}$$

This method is implemented in all principal languages (Matlab since 1996 [22], Arpack since 1998 [23]). It computes the eigenmodes according to the order of the largest time constants τ_i^F.

The set of eigenmodes $\hat{V}_i^F$ forms a basis for the subspace $H_F^1(\Omega) \subset H^1(\Omega)$, which corresponds to the space of solutions of the physical problem (13).

The eigenmodes are mutually-orthogonal according to a scalar product $< u, v >= \int_\Omega u c v \, \partial\Omega$:

$$\forall i \neq j, \quad < \hat{V}_i^F, \hat{V}_i^F >= \int_\Omega \hat{V}_i^F \, c_0 \, \hat{V}_j^F \, \partial\Omega = 0 \tag{18}$$

The magnitude of each mode is imposed by the chosen normalization:

$$V_i^F = \frac{\hat{V}_i^F}{\left(\int_\Omega \hat{V}_i^F \, c_0 \, \hat{V}_i^F \, d\Omega \right)^{1/2}} \tag{19}$$

The first orthogonality property is thus:

$$\forall i, j \in \mathbb{N}, \quad < V_i^F, V_j^F >= \int_\Omega V_i^F \, c_0 \, V_j^F \, \partial\Omega = \delta_{ij} \tag{20}$$

By choosing the eigenmode V_j^F as test function in Eq. (16), we have:

$$-\int_\Omega k_0 \overrightarrow{\nabla} V_i^F \cdot \overrightarrow{\nabla} V_j^F \, d\Omega - \int_\Gamma V_i^F \, h_0 \, V_j^F \, d\Gamma = z_i^F \int_\Omega V_i^F \, c_0 \, V_j^F d\Omega \tag{21}$$

The second orthogonality property is obtained by combining Eq. (20) and Eq. (21):

$$-\int_\Omega k_0 \overrightarrow{\nabla} V_i^F \cdot \overrightarrow{\nabla} V_j^F \, d\Omega - \int_\Gamma V_i^F \, h_0 \, V_j^F \, d\Gamma = z_i^F \, \delta_{ij} \tag{22}$$

We saw previously that the state equation has been obtained by the projection of the thermal problem on the reduced basis (Eq. (7)). In the case where the complete basis $\left(z_i^F \, , \, V_i^F \right)$ is used, we obtain:

$$\begin{aligned} &\forall \, j \in \mathbb{N}^\star, \\ &\quad \sum_{i=1}^{\infty} \left(\int_\Omega V_j^F \ c_0 \ V_i^F \, d\Omega \right) \ \frac{\partial x_i}{dt} = \\ &\qquad -\sum_{i=1}^{\infty} \left(\int_\Omega k_0 \overrightarrow{\nabla} V_j^F \cdot \overrightarrow{\nabla} V_i^F \, \partial\Omega + \int_\Gamma V_j^F \, h_0 \, V_i^F \, \partial\Gamma \right) \ x_i \\ &\qquad + \int_\Omega \pi \, V_j^F \, \partial\Omega \end{aligned} \tag{23}$$

Thanks to the orthogonality properties (Eqs. (20) and (22)), the state equations are fully decoupled:

$$\forall\, j \in \mathbb{N}^\star, \quad \frac{\partial x_j}{\partial t} = z_j^F\, x_j + \int_\Omega V_j^F\, \pi\, \partial\Omega \tag{24}$$

As we will see later, the reduced basis $\left(\tilde{z}_i^F\ ,\ \tilde{V}_i^F\right)$ is built from the complete basis $\left(z_i^F\ ,\ V_i^F\right)$, such as the orthogonality properties (Eqs. (20) and (22)) are preserved. The decoupled state equation (24) allows to obtain an immediate resolution.
The Fourier basis is valid for a linear thermal problem, with stationary parameters and with homogeneous boundary conditions, whatever the value of the thermal exchange coefficient $h_0(M)$.

In the particular case where $\forall M \in \Gamma, h_0 = 0$, we have the Neumann problem :

$$\left\{\begin{array}{lcl} \forall M \in \Omega & : & c_0 \dfrac{\partial T}{\partial t} = \overrightarrow{\nabla} \cdot (k_0 \overrightarrow{\nabla} T) + \pi \\ \forall M \in \Gamma & : & \overrightarrow{\nabla} T \cdot \overrightarrow{n} = 0 \end{array}\right. \tag{25}$$

It is associated to the Neumann eigenvalue problem :

$$\left\{\begin{array}{lcl} \forall M \in \Omega & : & \overrightarrow{\nabla} \cdot \left(k_0 \overrightarrow{\nabla} \hat{V}_i^N\right) = z_i^N\, c_0\, \hat{V}_i^N \\ \forall M \in \Gamma & : & \overrightarrow{\nabla} \hat{V}_i^N \cdot \overrightarrow{n} = 0 \end{array}\right. \tag{26}$$

The set of eigenvectors $\hat{V}_i^N$ forms a basis for the subspace $H_N^1(\Omega) \subset H^1(\Omega)$. They are characterized by a null heat flux on the boundaries (Figure 1.b).

4.1.2 The Dirichlet basis

We consider a Dirichlet problem characterized by the following equations:

$$\left\{\begin{array}{lcl} \forall M \in \Omega & : & c_0 \dfrac{\partial T}{\partial t} = \overrightarrow{\nabla} \cdot (k_0 \overrightarrow{\nabla} T) + \pi \\ \forall M \in \Gamma & : & T = 0 \end{array}\right. \tag{27}$$

This problem defines a particular space of solutions named Dirichlet space H_0^1, which is a subspace of the Hilbert space H^1.

Eigenvectors $\hat{V}_i^D(M)$ are obtained by the resolution of the following eigenvalue problem :

$$\left\{\begin{array}{lcl} \forall M \in \Omega & : & \overrightarrow{\nabla} \cdot \left(k_0 \overrightarrow{\nabla} \hat{V}_i^D\right) = z_i^D\, c_0\, \hat{V}_i^D \\ \forall M \in \Gamma & : & \hat{V}_i^D = 0 \end{array}\right. \tag{28}$$

The variational formulation writes as[4]:

$$\forall g \in H_0^1(\Omega), \quad -\int_\Omega k_0 \overrightarrow{\nabla} g \cdot \overrightarrow{\nabla} \hat{V}_j^D\, \partial\Omega = z_i \int_\Omega g\, c_0\, \hat{V}_i^D\, \partial\Omega \tag{29}$$

The set of eigenvectors V_i^D forms a basis for the Dirichlet subspace $H_0^1(\Omega) \subset H^1(\Omega)$. They are characterized by a null value on the boundaries, as shown in figure (1.c).

[4]The test function $g \in H_0^1(\Omega)$ has a null value on the boundaries. The integral term $\int_\Gamma g\, k\, \overrightarrow{\nabla} \hat{V}_i^D \cdot \overrightarrow{n} d\Gamma$ is thus null.

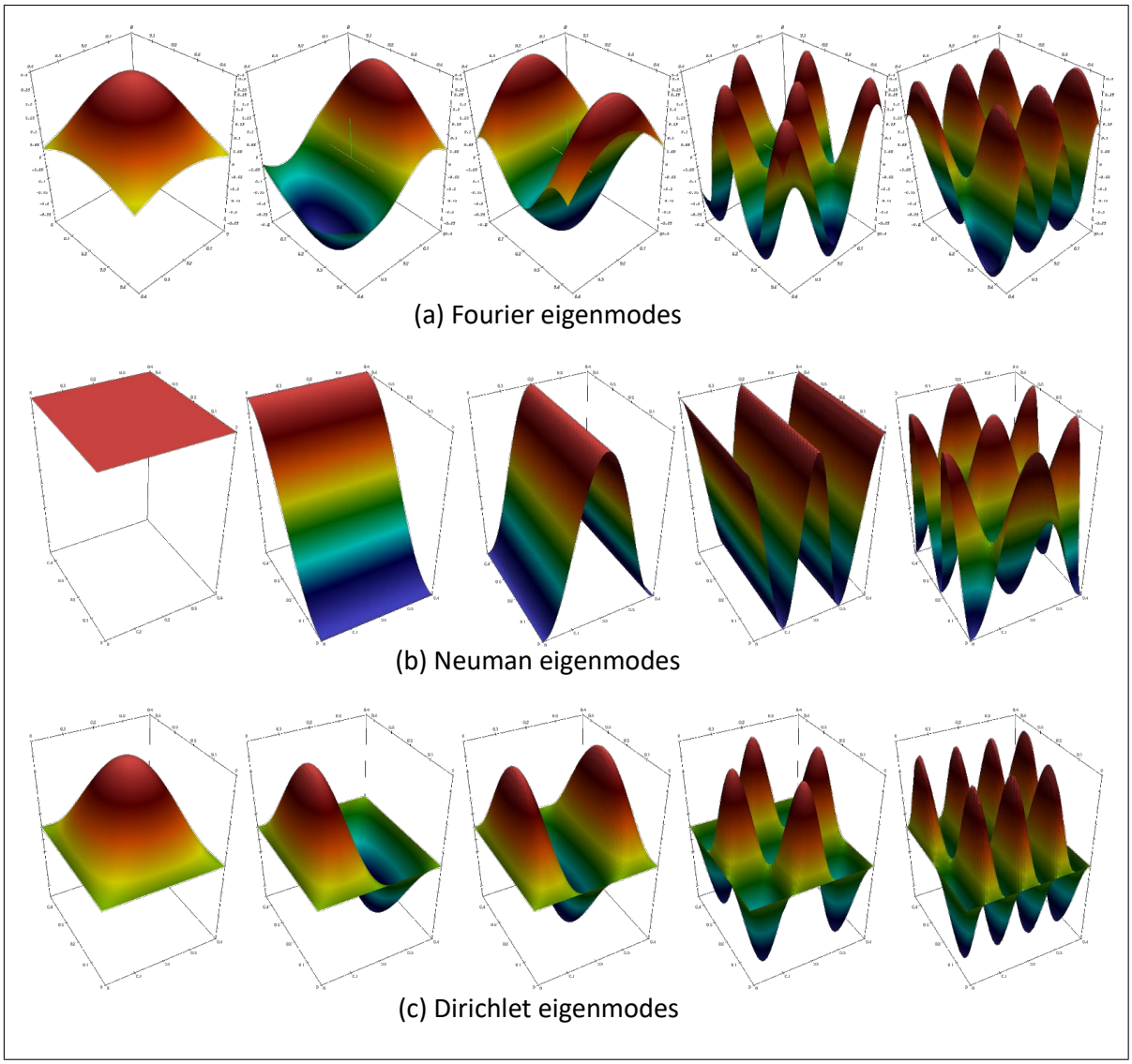

Figure 1: Classical modes for a simple 2D rectangular geometry

An adapted normalization[5] enables to fix the magnitude of the modes, and leads to the following orthogonality relations:

$$\forall\,(i,j)\in\mathbb{N}^{\star},\begin{cases}\displaystyle\int_{\Omega} V_i^D\; c_0\; V_j^D\;\partial\Omega=\delta_{ij}\\ \displaystyle\int_{\Omega} k_0\overrightarrow{\nabla}V_i^D\;\cdot\;\overrightarrow{\nabla}V_j^D\;d\Omega=z_i^D\;\delta_{ij}\end{cases}\tag{30}$$

4.1.3 Non homogeneous problem: applying a gliding temperature

We recall the general problem:

$$\begin{cases}\forall M\in\Omega \quad : \quad c_0\dfrac{\partial T}{\partial t}=\overrightarrow{\nabla}\cdot(k_0\overrightarrow{\nabla}T)+\pi\\ \forall M\in\Gamma \quad : \quad k_0\overrightarrow{\nabla}T\cdot\overrightarrow{n}=\varphi+h_0(T_f-T)\end{cases}\tag{31}$$

We saw that the Fourier eigenmodes defined by Eq. (14) form a basis for a thermal problem

[5] It is the same as the one used for the Fourier eigenmodes (Eq. (19))

characterized by homogeneous boundary conditions. In order to use the modal reduction with those eigenmodes, we have to split the temperature T into two terms :

$$T = T_g + T_d \tag{32}$$

- The term T_g is called the gliding temperature, because it corresponds to the temperature obtained without any consideration of the thermal inertia:

$$\begin{cases} \forall M \in \Omega & : & 0 = \overrightarrow{\nabla} \cdot (k_0 \overrightarrow{\nabla} T_g) + \pi \\ \forall M \in \Gamma & : & k_0 \overrightarrow{\nabla} T_g \cdot \overrightarrow{n} = \varphi + h_0 (T_f - T_g) \end{cases} \tag{33}$$

  Such a problem is simple: from the variational formulation Eq. (33):

$$-\int_\Omega k_0 \overrightarrow{\nabla} g \cdot \overrightarrow{\nabla} T_g \, d\Omega - \int_\Gamma g \, h_0 \, T_g \, d\Gamma + \int_\Omega g \, \pi \, d\Omega + \int_\Gamma g \, (\varphi + h_0 \, T_f) \, d\Gamma = 0 \tag{34}$$

  The discrete form is then:

$$\mathbf{A}\mathbf{T_g} + \mathbf{U}(t) = 0 \tag{35}$$

  leading to:

$$\mathbf{T_g} = -\mathbf{A}^{-1}\mathbf{U}(t) \tag{36}$$

- The complementary variable T_d is called the dynamic temperature. From Eqs. (31) and (33), T_d is solution of:

$$\begin{cases} \forall M \in \Omega & : & c_0 \dfrac{\partial T_d}{\partial t} = \overrightarrow{\nabla} \cdot (k_0 \overrightarrow{\nabla} T_d) - c_0 \dfrac{\partial T_g}{\partial t} \\ \forall M \in \Gamma & : & k_0 \overrightarrow{\nabla} T_d \cdot \overrightarrow{n} = -h_0 \, T_d \end{cases} \tag{37}$$

  Such a problem is homogeneous and it can be reduced with the Fourier basis.

Lastly the researched temperature field T is:

$$T = \sum_{i=1}^{\infty} x_i \, V_i^F + T_g \tag{38}$$

The state modal problem remains decoupled. The gliding temperature T_g appears only if the solicitations are time-dependent:

$$\forall i \in \mathbb{N}^\star, \quad \frac{dx_i}{dt} = z_i \, x_i - \int_\Omega V_i^F \, c_0 \frac{dT_g}{dt} d\Omega \tag{39}$$

Several studies have used this technique, including buildings problems [24, 25, 26, 27].

However, the limit of this method is that the computed basis is applicable only for problems in which the boundary conditions are fixed. From the second equation of (14), we can define the quantity γ_i such as:

$$\gamma_i = \frac{\overrightarrow{\nabla} V_i \cdot \overrightarrow{n}}{V_i} = \frac{-h_0}{k_0} \tag{40}$$

Every eigenvector is characterized by the same value of γ_i. Thus, all the dynamic thermal fields that can be rebuilt by this modal formulation will respect this constraint.
Such bases are not compatible with a thermal problem in which non linearities or time variations exist on the boundaries. Examples are numerous: time-dependent exchange coefficient $h(t)$, thermal conductivity depending on the temperature $k(T)$, infrared radiations... That is why other bases have been developed.

4.2 Basis adapted to non linear problems

4.2.1 Branch modes

In order to overcome this limitation, a new basis is defined, whose boundary conditions are not linked to the physical boundary conditions:

$$\begin{cases} \forall M \in \Omega \quad , \quad \overrightarrow{\nabla} \cdot \left(k_0 \overrightarrow{\nabla} \hat{V}_i^B \right) = z_i^B \, c_0 \, \hat{V}_i^B \\ \forall M \in \Gamma \quad , \quad k_0 \overrightarrow{\nabla} \hat{V}_i^B \cdot \overrightarrow{n} = -z_i^B \, \zeta \, \hat{V}_i^B \end{cases} \tag{41}$$

The main feature of this basis is that the eigenvalue z_i^B is present in the boundary condition. This is the Steklov condition.
The quantity ζ [J.m^{-2}K^{-1}] is called Steklov parameter and it is a simple coefficient which grants the respect of the physical dimensions in the boundary condition equations. The value of this coefficient is obtained from the variational formulation of the eigenvalue problem (41).

$$- \int_\Omega k_0 \overrightarrow{\nabla} g \cdot \overrightarrow{\nabla} V_i^B \, d\Omega = z_i \left(\int_\Omega c_0 \, g \, V_i^B \, d\Omega + \int_\Gamma \zeta \, g \, V_i^B \, d\Gamma \right) \tag{42}$$

To balance the two terms linked to the eigenvalue, an appropriate choice of the Steklov coefficient ζ is given by:

$$\zeta \simeq \frac{\displaystyle\int_\Omega c_0 \, d\Omega}{\displaystyle\int_\Gamma d\Gamma} \tag{43}$$

Using the associated scalar product:

$$< u, v >= \int_\Omega u \, c_0 \, v \, d\Omega + \int_\Gamma u \, \zeta \, v \, d\Gamma \tag{44}$$

the normalization is done:

$$V_i^B = \frac{\hat{V}_i^B}{\left(\displaystyle\int_\Omega \hat{V}_i^B \, c_0 \, \hat{V}_i^B \, d\Omega + \int_\Gamma \hat{V}_i^B \, \zeta \, \hat{V}_i^B \, d\Gamma \right)^{1/2}} \tag{45}$$

and we obtain the following orthogonality properties:

$$\begin{aligned} &\forall (i,j) \in \mathbb{N}^\star, \\ &\int_\Omega V_j^B \, c_0 \, V_i^B \, d\Omega + \int_\Gamma V_i^B \, \zeta \, V_i^B \, d\Gamma = \delta_{ij} \\ &\int_\Omega k_0 \overrightarrow{\nabla} V_j^B \cdot \overrightarrow{\nabla} V_i^B \, d\Omega = z_i^B \, \delta_{ij} \end{aligned} \tag{46}$$

It is possible to characterize the spatial evolution of each branch modes by defining a localization coefficient C_i^ζ for each mode V_i^B:

$$C_i^\zeta = \int_\Gamma V_i^B \, \zeta \, V_i^B \, d\Gamma \tag{47}$$

The evolution of this coefficient with the mode number, for a simple rectangular geometry, is presented in figure 2. It shows that two families of branch modes exist:

- Because of the orthogonality relation defined in Eq. (14), when C_i^ζ is close to 1, the considered mode is flat on the domain except near the border. Such modes are called boundary modes. They do not appear in a classical Fourier basis, and allow the reconstitution of any boundary conditions.
- Other modes exist. Their spatial evolutions are located in the core of the domain. We call them domain modes. Those modes are characterized by a weak value of c_i^ζ (less than 0.3 for the example in figure 2).

Figure 3.a presents some branch modes for a simple 2D rectangular geometry. This figure enables to clearly visualize these two families of branch modes.

With the branch modes, the orthogonality properties do not allow to obtain a decoupled modal problem anymore:

$$\begin{aligned} \forall j \in \mathbb{N}^\star, \quad & \sum_{i=1}^{\infty} \left(\int_\Omega V_j^B \, c \, V_i^B \, d\Omega \right) \frac{dx_i}{dt} \\ & = - \sum_{i=1}^{\infty} \left(\int_\Omega k \overrightarrow{\nabla} V_j^B \cdot \overrightarrow{\nabla} V_i^B \, d\Omega + \int_\Gamma V_j^B \, h \, V_i^B \, d\Gamma \right) x_i \\ & + \int_\Omega V_j^B \, \pi \, d\Omega + \int_\Gamma V_j^B \, (hT_e + \varphi) d\Gamma \end{aligned} \tag{48}$$

This is the price to pay for using this basis. On the other hand, the branch modes form a basis for any thermal problem, including those characterized by parameters that are functions of time or temperature. It is demonstrated that the generated functional space is the Hilbert space $H^1(\Omega)$ and we have directly[6]:

$$T(M,t) = \sum_{i=1}^{\infty} x_i \, V_i^B \tag{49}$$

Initiated by Neveu *et al.* [28], this basis has been applied to different configurations: Quéméner *et al.* [29] treated the case of a non-linear problem, with the existence of solidification of a molded part. Various applications were made for inverse problems by Videcoq *et al.* [30, 31, 32]. A generalization of Branch bases to advection-diffusion problem has been proposed by Joly *et al.* [33], then used in the case of an inverse problem of identification [34]. Finally Laffay *et al.* [35, 36] proposed a sub-structuring technique, that allows the computation of branch bases for different subdomains, which are then coupled by a thermal contact resistance.

4.2.2 The Dirichlet-Steklov eigenmodes

Recently another way to reduce non linear problems with or without time-dependent parameters has been developed. It consists in using two bases:

- the Dirichlet basis previously presented (Eq. (27)),
- the Steklov basis[7], which is defined by the following eigenvalue problem:

$$\begin{cases} \forall M \in \Omega \quad , \quad \overrightarrow{\nabla} \cdot (k_0 \overrightarrow{\nabla} \hat{V}_i^S) = 0 \\ \forall M \in \Gamma \quad , \quad k_0 \overrightarrow{\nabla} \hat{V}_i^S \cdot \overrightarrow{n} = -z_i^S \, \zeta \, \hat{V}_i^S \end{cases} \tag{50}$$

[6] It is no longer necessary to use the gliding temperature field

[7] Steklov modes are rigorously defined only on the boundaries. In order to simplify the notation, we denote here by abuse of language Steklov modes as their harmonic lifting in the domain (noted $\hat{V}_i^S$)

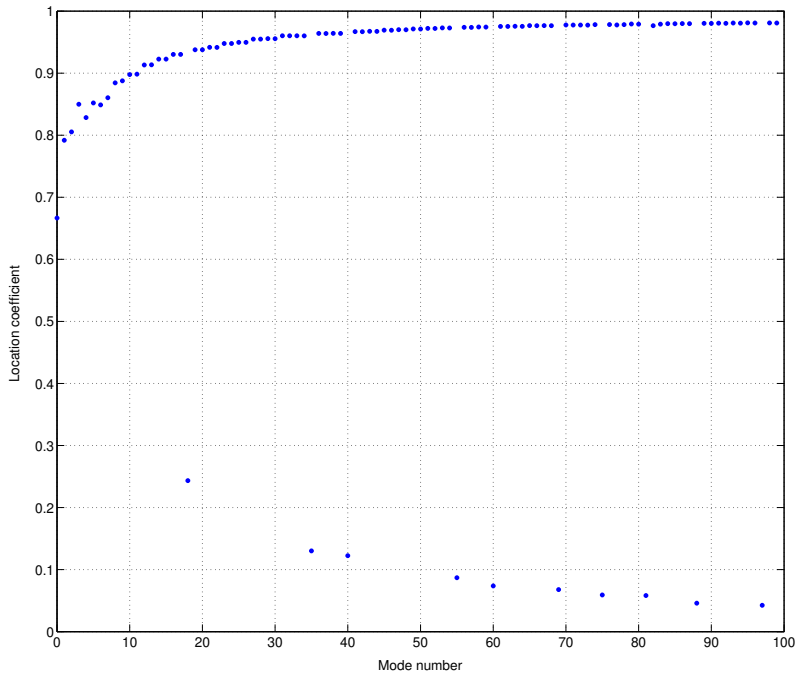

Figure 2: Evolution of the location coefficient according to the branch mode number

Steklov modes correspond to stationary fields obtained for a problem in which the imposed heat flux density at the boundaries is proportional to the value of the mode at any point on the border.

The union of these two bases $\{V_i^D\}_{i\in\mathbb{N}} \bigoplus \{V_j^S\}_{j\in\mathbb{N}}$ forms a Hilbert base of $H^1(\Omega)$. We define the following scalar product:

$$< u, v >= \int_\Omega k_0 \overrightarrow{\nabla} u \ \cdot \ \overrightarrow{\nabla} v \, d\Omega + z_0 \int_\Gamma u \, \zeta \, v \, d\Gamma \tag{51}$$

where z_0 is a constant parameter $[s^{-1}]$ which allows to respect the physical dimension of both terms.

Using the following normalization:

$$V_i^S = \frac{\hat{V}_i^{DS}}{\left(\int_\Omega k_0 \overrightarrow{\nabla} \hat{V}_i^{DS} \ \cdot \ \overrightarrow{\nabla} \hat{V}_i^{DS} \, d\Omega + z_0 \int_\Gamma \hat{V}_i^{DS} \, \zeta \, \hat{V}_i^{DS} \, d\Gamma \right)^{1/2}} \tag{52}$$

we obtain Dirichlet and Steklov modes which are orthogonal with respect to this scalar product (51):

$$\begin{aligned} \forall \mathcal{X}, \mathcal{Y} \in \{D, S\}, \forall (i,j) \in \mathbb{N}^\star, & \\ < \hat{V}_i^{\mathcal{X}}, \hat{V}_j^{\mathcal{Y}} > \ &= \int_\Omega k_0 \overrightarrow{\nabla} \hat{V}_i^{\mathcal{X}} \ \cdot \ \overrightarrow{\nabla} \hat{V}_j^{\mathcal{Y}} \, d\Omega + z_0 \int_\Gamma \hat{V}_i^{\mathcal{X}} \, \zeta \, \hat{V}_j^{\mathcal{Y}} \, d\Gamma \\ &= \delta_{\mathcal{X}\mathcal{Y}} \, \delta_{ij} \end{aligned} \tag{53}$$

Examples of Dirichlet-Steklov modes are compared to the Branch modes in Fig. 3. Steklov modes correspond very well to boundary branch modes, whereas domain branch modes and Dirichlet modes are similar only inside the domain. At the boundaries, domain branch modes are not characterized by null values, unlike Dirichlet modes. Nevertheless the correspondence between these two bases is obvious.

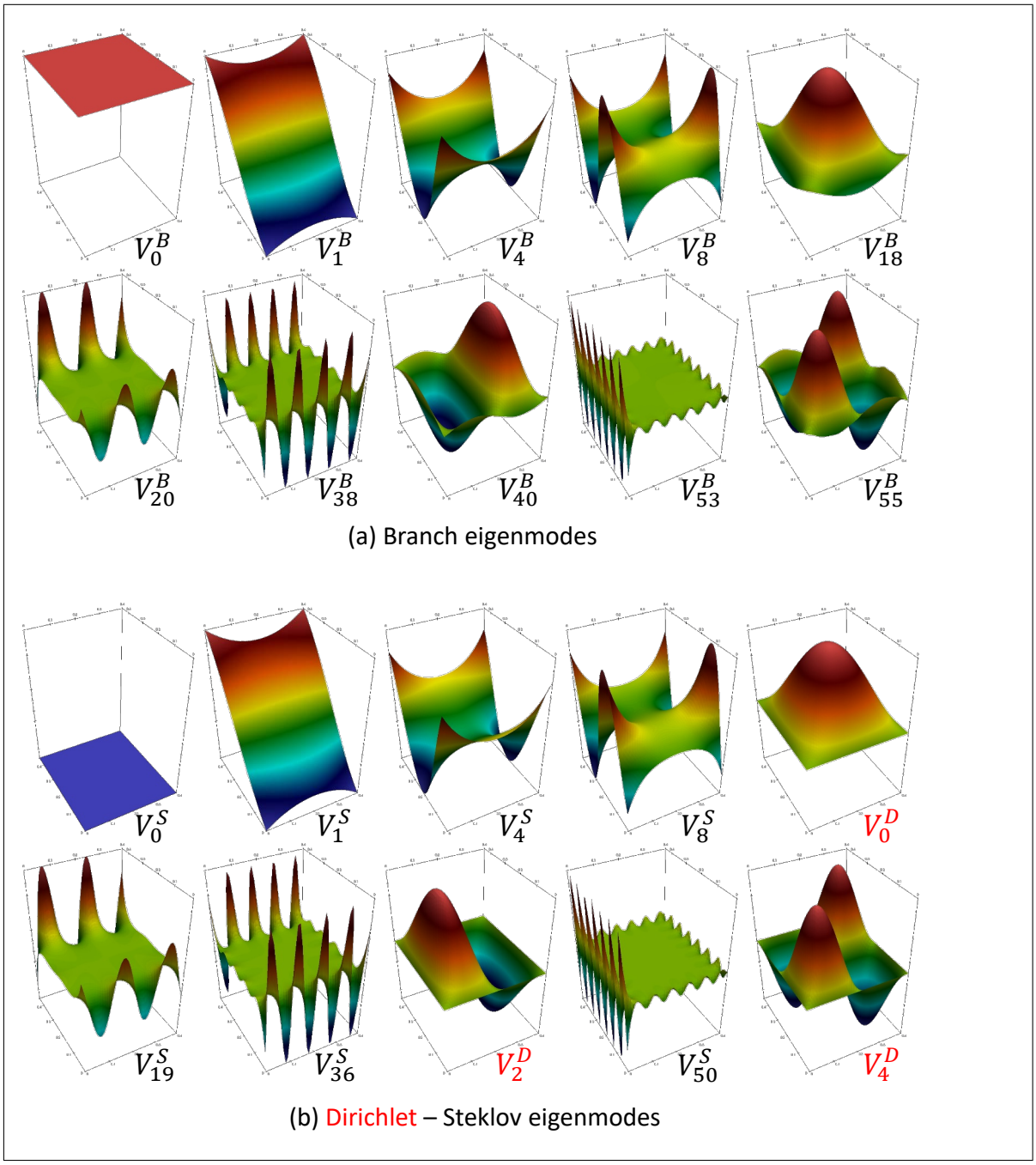

Figure 3: Comparison between the Branch basis $\{V_i^B\}$ and the Dirichlet-Steklov basis $\{V_i^D\} \bigoplus \{V_j^S\}$

5 Basis reduction

Until now, no reduction has been made. Whatever the chosen basis, the state problem (Eq. (39) or (48)) remains characterized by a dimension related to spatial discretization. The second step of the AROMM method is to build a reduced base of n modes $\tilde{V}_i(M)$ from the complete base. We saw previously that the form of the reduced modal problem depends on the chosen basis:

- For a basis associated with a linear thermal problem and with stationary parameters (*i.e.* Fourier basis $\{V_i^F\}$, Neumann basis $\{V_i^N\}$ or Dirichlet basis $\{V_i^D\}$):

$$\forall i \in \{1,n\} \quad \frac{dx_i}{dt} = z_i\, x_i - \int_\Omega \tilde{V}_i\, c_0\, \frac{dT_g}{dt} d\Omega \tag{54}$$

- For a basis adapted to more general problems (*i.e.* Branch basis $\{V_i^B\}$ or Dirichlet-Steklov basis $\{V_i^D\} \bigoplus \{V_j^S\}$):

$$\begin{aligned} \forall j \in \{1,n\} \quad & \sum_{i=1}^{n} \left(\int_\Omega \tilde{V}_j\, c\, \tilde{V}_i\, d\Omega \right) \dot{x}_i \\ & = -\sum_{i=1}^{n} \left(\int_\Omega k \vec{\nabla} \tilde{V}_j \cdot \vec{\nabla} \tilde{V}_i\, d\Omega + \int_\Gamma \tilde{V}_j\, h\, \tilde{V}_i\, d\Gamma \right) x_i \\ & + \int_\Omega \tilde{V}_j\, \pi\, d\Omega + \int_\Gamma \tilde{V}_j\, (h\, T_e + \varphi)\, d\Gamma \end{aligned} \tag{55}$$

Several reduction methods exist.

5.1 Truncation

The simplest idea is to take the most relevant modes from the complete base:

$$\forall i \in \{1,n\} \quad \forall j \in \{1,N\} \quad , \quad \tilde{V}_i = V_j \tag{56}$$

5.1.1 Temporal Truncation

A first criterion leads to the truncation of Marshall [37]. In this method the modes with the largest time constant are kept. Independent of any reference problem, this reduction technique has mostly been used for classical bases [38].

The advantage of this reduction is that it is immediate to use, since the Lanczos technique allows to calculate the basis according to the order of the largest time constant. Thus, temporal truncation can also be used as first-level reduction: instead of calculating the complete basis, only a certain percentage of this basis is computed, from which it is possible to make a second and more efficient reduction. In the case of problems characterized by a very large number of DOF, the possibility to compute a small part of the basis is of great interest, bacause of the large calculation times needed for solving the eigenvalue problem and the difficulties of the eigenvectors storage.

5.1.2 Energetic Truncation

This technique is used by Joly *et al.* [33]. From a set of known temperature fields $T_{ref}(t)$, the excitation states are obtained by a simple projection of $T_{ref}(t)$ on the complete basis

according to the appropriate scalar product.

For example, in the case of the branch basis, orthogonal properties lead to:

$$\begin{aligned}
&\forall j \in \{1,n\},\\
&\int_\Omega T_{ref}\, c_0\, V_j^B\, d\Omega + \int_\Gamma T_{ref}\, \zeta\, V_j^B\, d\Gamma\\
&\qquad = \int_\Omega \sum_{i=1}^{n} \left(x_i\, V_i^B\right) c_0\, V_j^B\, d\Omega + \int_\Gamma \sum_{i=1}^{n} \left(x_i\, V_i^B\right)\, \zeta\, V_j^B\, d\Gamma\\
&\qquad = \sum_{i=1}^{n} \left(\int_\Omega V_i^B\, c_0\, V_j^B\, d\Omega + \int_\Gamma V_i^B\, \zeta\, V_j^B\, d\Gamma \right) x_i\\
&\qquad = \sum_{i=1}^{n} \delta_{ij} x_i\\
&\qquad = x_j
\end{aligned} \tag{57}$$

For the Dirichlet-Steklov basis, the definition of the scalar product leads to:

$$\begin{aligned}
&\forall \mathcal{X},\mathcal{Y} \in \{D,S\}, \forall j \in \{1,n\},\\
&\int_\Omega k_0 \overrightarrow{\nabla} T_{ref} \cdot \overrightarrow{\nabla} \hat{V}_j^{\mathcal{Y}}\, d\Omega + \int_\Gamma T_{ref}\, \zeta\, \hat{V}_j^{\mathcal{Y}}\, d\Gamma\\
&\qquad = \int_\Omega k_0 \overrightarrow{\nabla} \left(\sum_{i=1}^{n} x_i\, \hat{V}_i^{\mathcal{X}} \right) \cdot \overrightarrow{\nabla} \hat{V}_j^{\mathcal{Y}}\, d\Omega + \int_\Gamma \left(\sum_{i=1}^{n} x_i\, \hat{V}_i^{\mathcal{X}} \right) \zeta\, \hat{V}_j^{\mathcal{Y}}\, d\Gamma\\
&\qquad = \sum_{i=1}^{n} \left(\int_\Omega k_0 \overrightarrow{\nabla} \hat{V}_i^{\mathcal{X}} \cdot \overrightarrow{\nabla} \hat{V}_j^{\mathcal{Y}}\, d\Omega + \int_\Gamma \hat{V}_i^{\mathcal{X}}\, \zeta\, \hat{V}_j^{\mathcal{Y}}\, d\Gamma \right) x_i\\
&\qquad = \sum_{i=1}^{n} \delta_{\mathcal{X}\mathcal{Y}}\, \delta_{ij}\, x_i\\
&\qquad = x_j
\end{aligned} \tag{58}$$

The knowledge of the excitation state of every mode of the complete basis enables to keep only those with the largest state value. This technique generally leads to a more efficient reduction than the simple temporal truncation, but it has two disadvantages. First, the performance of the reduction depends on the reference fields. Second, the reference fields have to be computed, which might be difficult. Here we find the same constraints as those existing for the POD method. From the same discretized geometry it is generally possible to perform simulations of a thermal problem simpler than the one studied, but which will however trigger the characteristic modes.

5.2 Amalgamated base

The amalgam is a more elaborate technique. It retains the idea of classifying eigenmodes according to their excitation states, but this time the modes that are discarded during the truncation are added to the retained modes by simple linear combinations:

$$\forall i \in \{1,n\} \quad \tilde{V}_i = V_{i,1} + \sum_{p=2}^{\tilde{N}_i} \alpha_{i,p} V_{i,p} \quad ; \quad 0 < |\alpha_{i,p}| < 1 \tag{59}$$

In order to maintain the orthogonality properties of the basis, each mode is used only once:

$$\sum_{i=1}^{n} \tilde{N}_i = N \tag{60}$$

The distribution of the initial modes and the computation of the amalgam coefficients $\alpha_{i,p}$ are carried out in a fast sequential procedure which depends only on the knowledge of the excitation states. Set up by Oulefki [39] in the case of classical bases for which the decoupling facilitates the determination of the reference states, this reduction technique has been widely used for branch modes.
In general, the difficulty lies in finding the excitation states of the complete basis. A first rather simple solution [40, 41] is, as for energetic truncation, to use a set of temperature fields obtained by complete solution of a reference problem, which gives access to the excitation states (Eq. (57) or (58)).
Other techniques have also been tested [29, 31, 35] in order to avoid computing the reference thermal fields. Since the excitation states are only needed to classify modes to set up the amalgam procedure, these authors have built the associated complete modal problem, and sought a simple estimate of the states of excitation: Using a branch basis and neglecting the coupling between modes, the modal problem has been solved analytically and the excitation states were readily obtained [29]. An improvement of this technique has been carried out in the case of a rotating disc, for which only the coupling of a small number of modes was considered [42].

6 Application to the inverse problems: Examples

The examples presented here concern an automotive brake system, which is a major safety component. It undergoes, during its operating phase, many mechanical and thermal stresses, which can lead to important damages: cracks, apparition of hot-judder, vapor locking, brake fade, etc.
Because thermal solicitations are rarely known (especially the part of the heat flux received by the pad and by the disc), an inverse technique is used. In order to respect the geometry of the system, the models used in the inverse process are numerical, and characterized by very fine meshes. As computing time and memory problems appear very quickly, reduced models are employed.

6.1 Estimation of heat flux received by a rotating brake disc

A brake disc in rotation with variable rotation frequency $\omega(t)$ is considered (Fig. 4). During the braking phase, the disc receives a time-dependent heat flux on the zone of friction with the brake pads Ω_1. The flux density $\varphi[W.m^{-2}]$ dissipated by friction is not uniform but varies linearly with the velocity and thus with the radius.
The space discretization using P1 finite elements leads to a number of DOF $N = 9860$ for the following matrix formulation:

$$\mathbf{C}\frac{d\mathbf{T}}{dt} = [\mathbf{K} + \omega_u(t)\mathbf{U} + h_u(t)\mathbf{H}]\,\mathbf{T} + \varphi_u\mathbf{U} \tag{61}$$

The goal consists in identifying $\varphi_u(t)$ in real time, from a local infrared measurement on the disc (point A).
Concerning the direct simulation, the computing time is significant (equal to 2160 s on a simple laptop), because the transport term involves small computation time-steps. Figure 5 illustrates this phenomenon.
Such simulation time is an obstacle for inverse applications where the need for real-time response is important. To avoid prohibitive time, a reduced model is built. It is obtained by

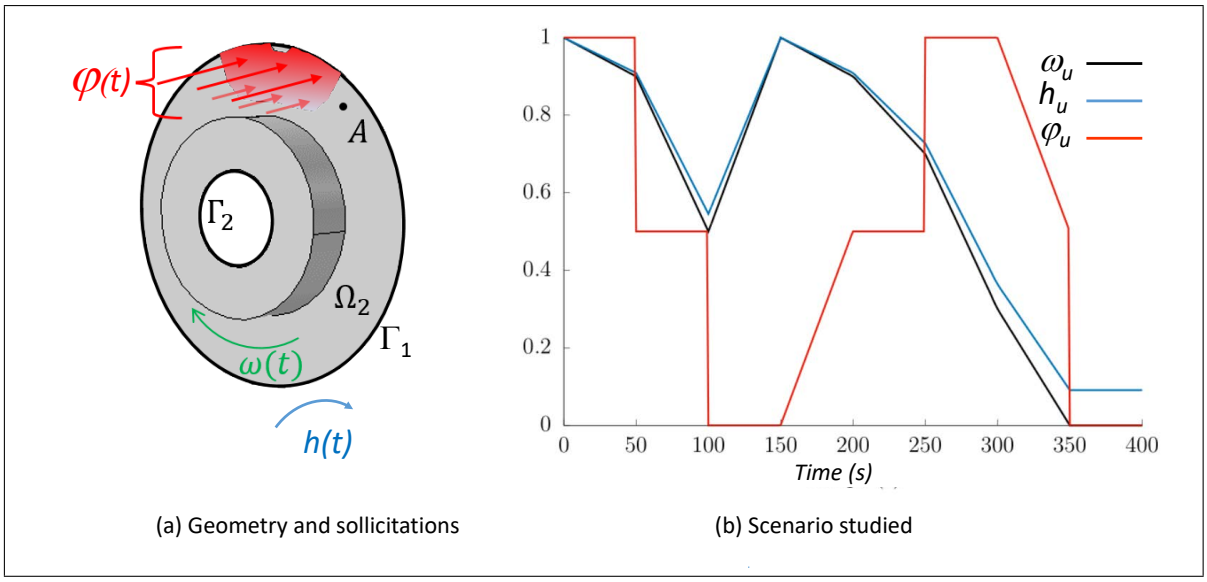

Figure 4: Physical problem

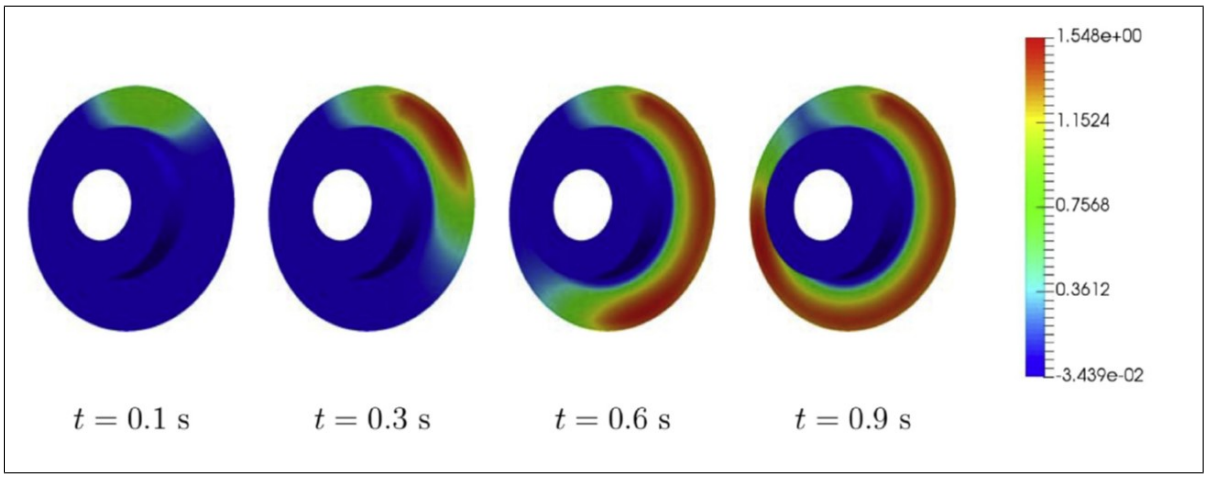

Figure 5: Temperature fields at different times

the AROMM method with branch eigenmodes (Fig. 6.a). The reference scenario used for the amalgam procedure (Fig. 6.b) is obviously different from the one used for the identification (Fig. 4.b). With a reduced order $n = 15$, the direct simulation requires less than 10s, with satisfying results (Fig. 7).
By integrating such reduced model in an inverse approach, it is possible to identify the heat flux φ in quasi real time. The inverse algorithm is based on the adjoint method applied on sliding time windows (Fig. 8).

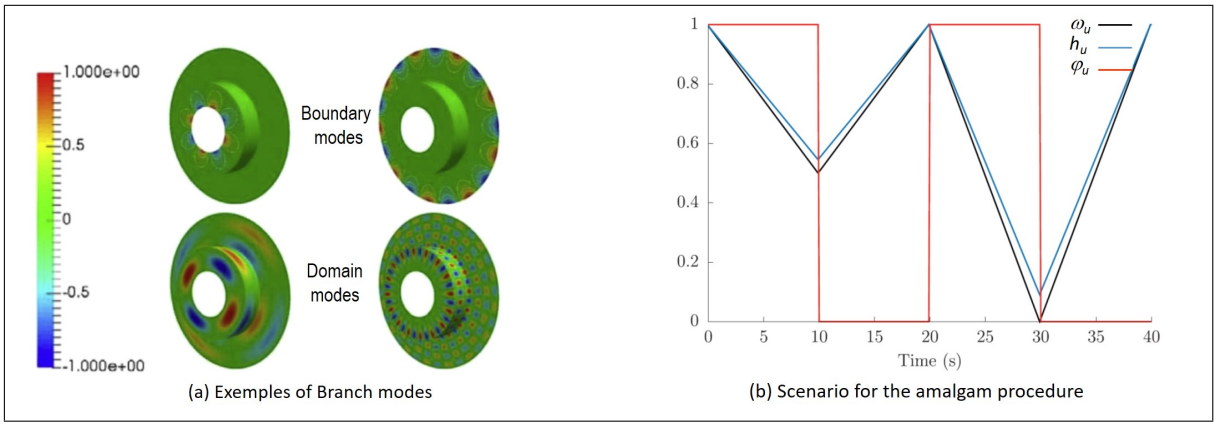

(a) Exemples of Branch modes (b) Scenario for the amalgam procedure

Figure 6: Reduced model

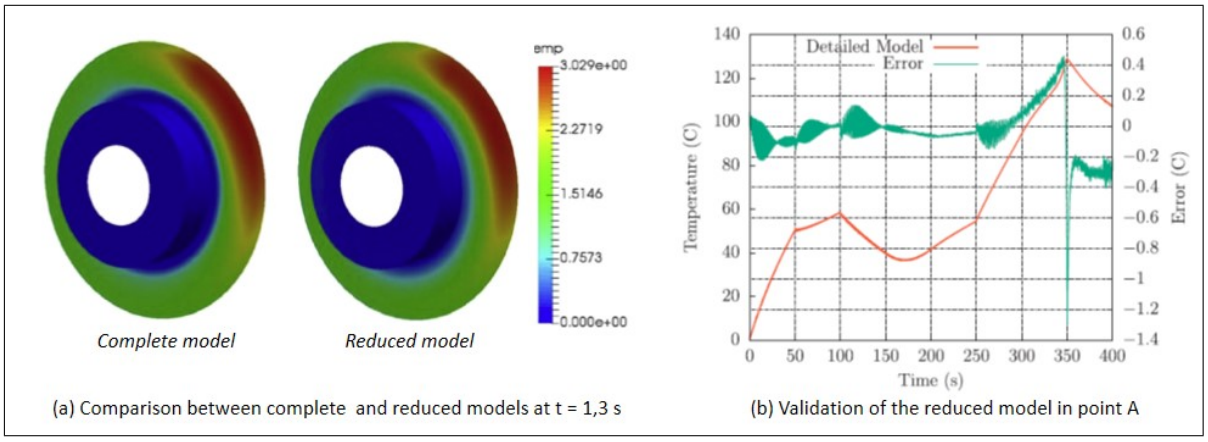

(a) Comparison between complete and reduced models at t = 1,3 s (b) Validation of the reduced model in point A

Figure 7: Using the reduced model $\tilde{n} = 15$ in direct simulation

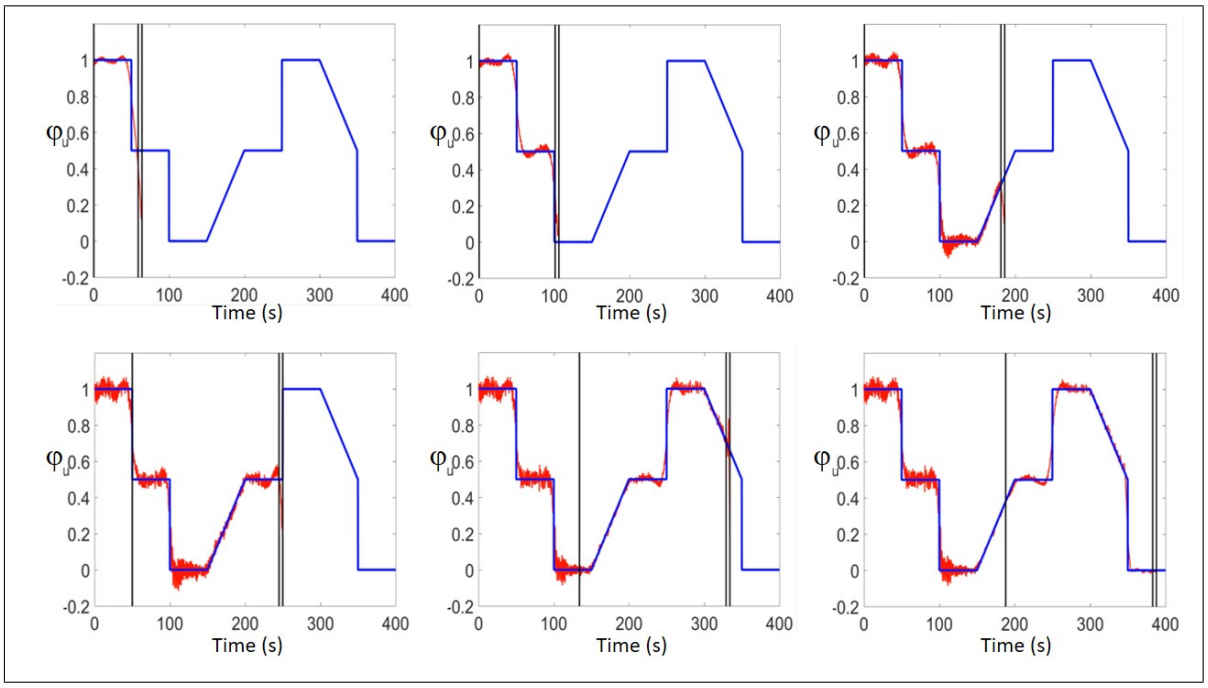

Figure 8: Identification results

6.2 Spatio-temporal identification of a heat flux density field received by a brake pad

The application relates to the identification of the heat flux received by a brake pad in a braking situation, for which the mechanical deformation and the phenomena of tear and wear cause the appearance of hot spots that one seeks to locate.
We consider a brake pad for which the complexity of the geometry is respected (Fig. 9.a). It is composed of two materials: the brake lining and its metallic support. This brake pad undergoes three types of boundary conditions (Fig. 9.b).

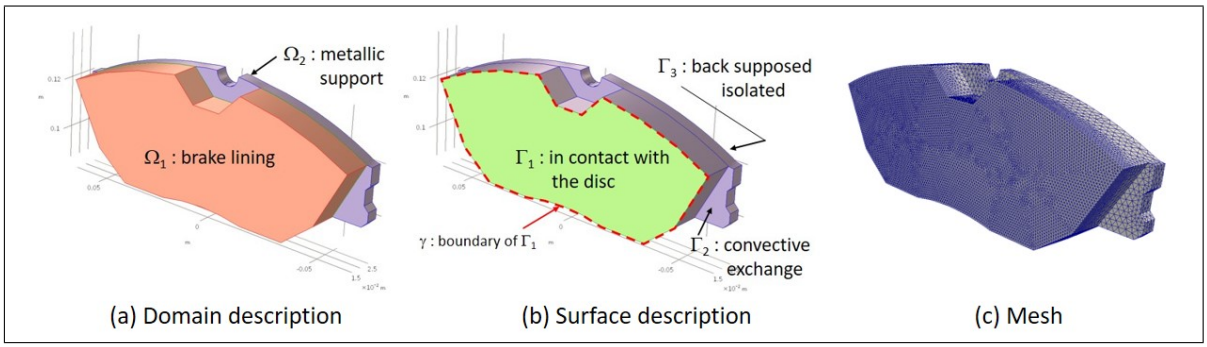

Figure 9: Geometry of the pad and its discretization

6.2.1 Parametrization of the heat flux density

A first branch base $V^{(\varphi)}$ is used in order to parametrize the heat flux density (Fig. 10):

$$\varphi(x,y,t) = \sum_{k=1}^{n^{(\varphi)}} \tilde{x}_k^{(\varphi)}(t)\, \tilde{V}_k^{(\varphi)}(x,y) \tag{62}$$

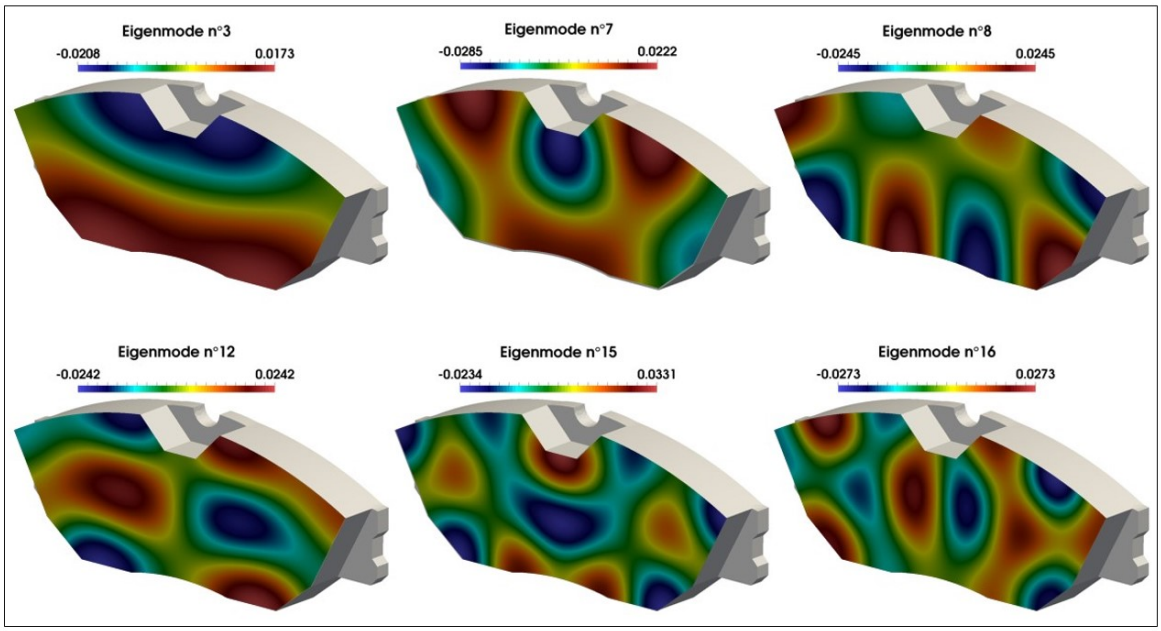

Figure 10: Flux basis

The discretization of the heat equation (Eq. (3)) leads to:

$$\mathbf{C}\dot{\mathbf{T}} = (\mathbf{K}+\mathbf{H})\mathbf{T} + \sum_{k=1}^{n^{(\varphi)}} \mathbf{W}\,\tilde{\mathbf{V}}_k^{(\boldsymbol{\varphi})}\,\tilde{x}_k^{(\varphi)} \tag{63}$$

where $\tilde{\mathbf{V}}_k^{(\boldsymbol{\varphi})}$ $[N_{mesh}]$ is the extension on the domain Ω of each eigenvector $\tilde{V}_k^{(\varphi)}$ computed on the boundary Γ_1, and where the matrix $\mathbf{W}$ $[N_{mesh} \times N_{mesh}]$ corresponds to the integration of the interpolations functions defined on the border Γ_1 and extended to the domain Ω.
This can be written compactly:

$$\mathbf{C}\dot{\mathbf{T}} = (\mathbf{K}+\mathbf{H})\mathbf{T} + \mathbf{W}\,\tilde{\mathbf{V}}^{(\boldsymbol{\varphi})}\,\tilde{\mathbf{X}}^{(\boldsymbol{\varphi})} \tag{64}$$

where $\tilde{\mathbf{V}}^{(\boldsymbol{\varphi})}$ is a matrix of dimension $[N_{mesh} \times n^{(\varphi)}]$ which gathers all the flux modes $\tilde{\mathbf{V}}_k^{(\boldsymbol{\varphi})}$ $[N_{mesh}]$ used, and $\tilde{\mathbf{X}}^{(\boldsymbol{\varphi})}$ is the vector of the corresponding states of dimension $[n^{(\varphi)}]$.

6.2.2 Reduced problem

A second branch base V^T is used for the temperature field (Fig. 11)

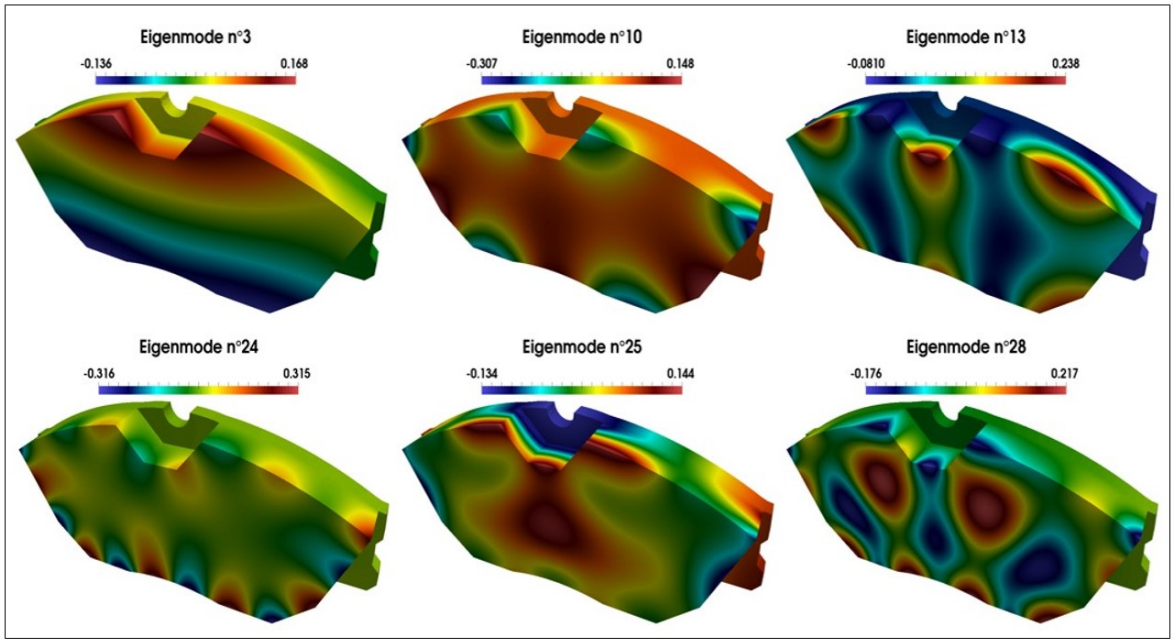

Figure 11: Temperature basis

The reduced modal expression of the thermal problem defined by equation (10) is then:

$$\mathbf{L}\dot{\tilde{\mathbf{X}}}^{(\mathbf{T})} = \mathbf{M}\,\tilde{\mathbf{X}}^{(\mathbf{T})} + \mathbf{D}\,\tilde{\mathbf{X}}^{(\boldsymbol{\varphi})} \tag{65}$$

with $\mathbf{D} = \tilde{\mathbf{V}}^{(\mathbf{T})t}\ \mathbf{W}\ \tilde{\mathbf{V}}^{(\boldsymbol{\varphi})}$

6.2.3 Spatio-temporal identification

We thus have a temperature model characterized by a few dozens of excitation states of temperature x^T (instead of 67, 353 degrees of freedom of the initial mesh), to identify a few dozens of excitation states of flux x^{φ}, instead of the 5, 945 degrees of freedom of the surface $\Gamma 1$. The developed technique uses an iterative method of conjugate gradient descent, in which the gradient is estimated by the adjoint method.

The obtained results (Figures 12 and 13) are satisfactory. It can be noted that no specific regularization technique is used in this study (Tikhonov for example). Indeed, in addition to the natural regularization due to a whole time-domain approach and an iterative method, an additional regularization appears, induced by the two reductions (one for the thermal problem and another for the heat flux parametrization).

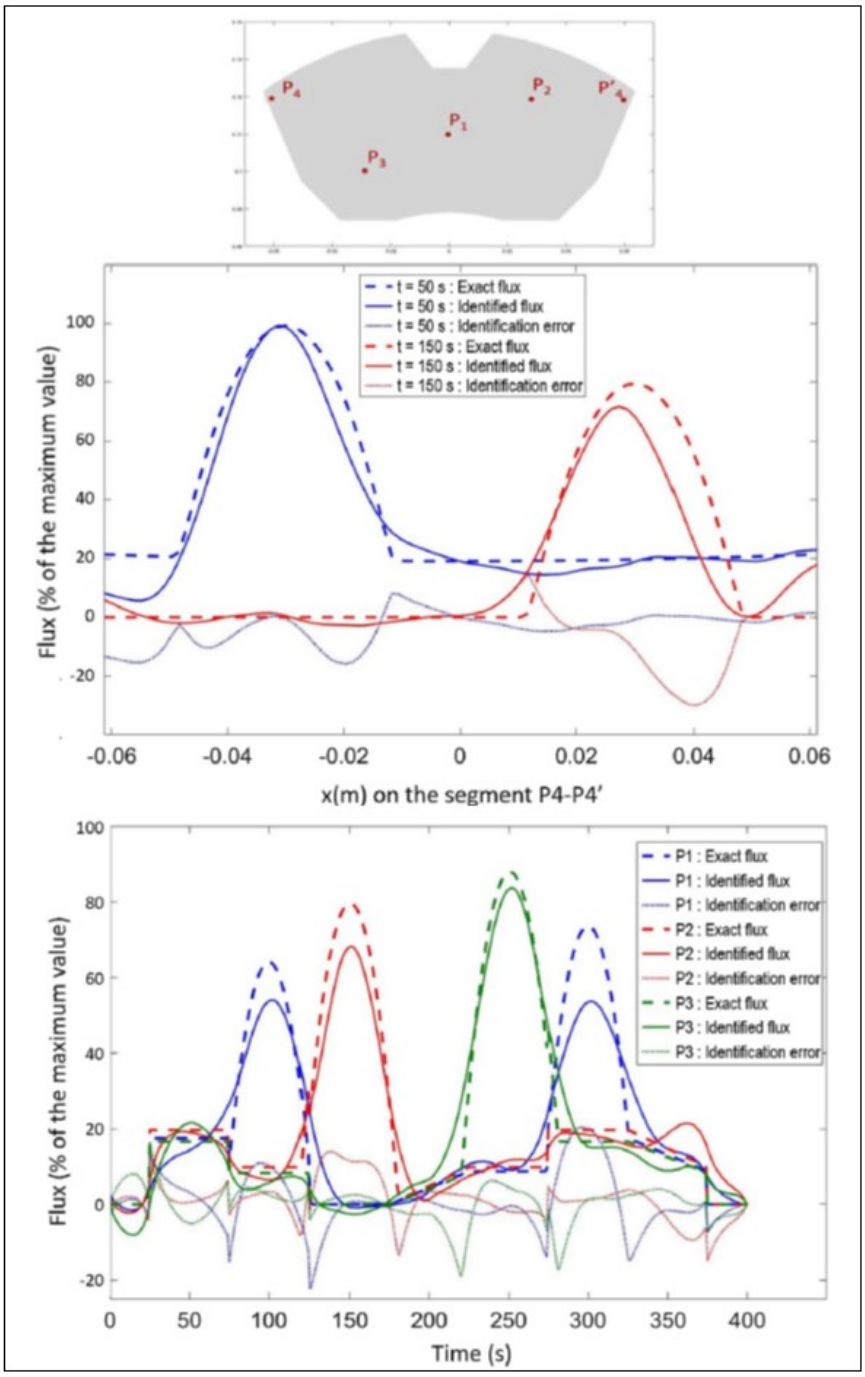

;

Figure 12: Identification results along a segment or versus time

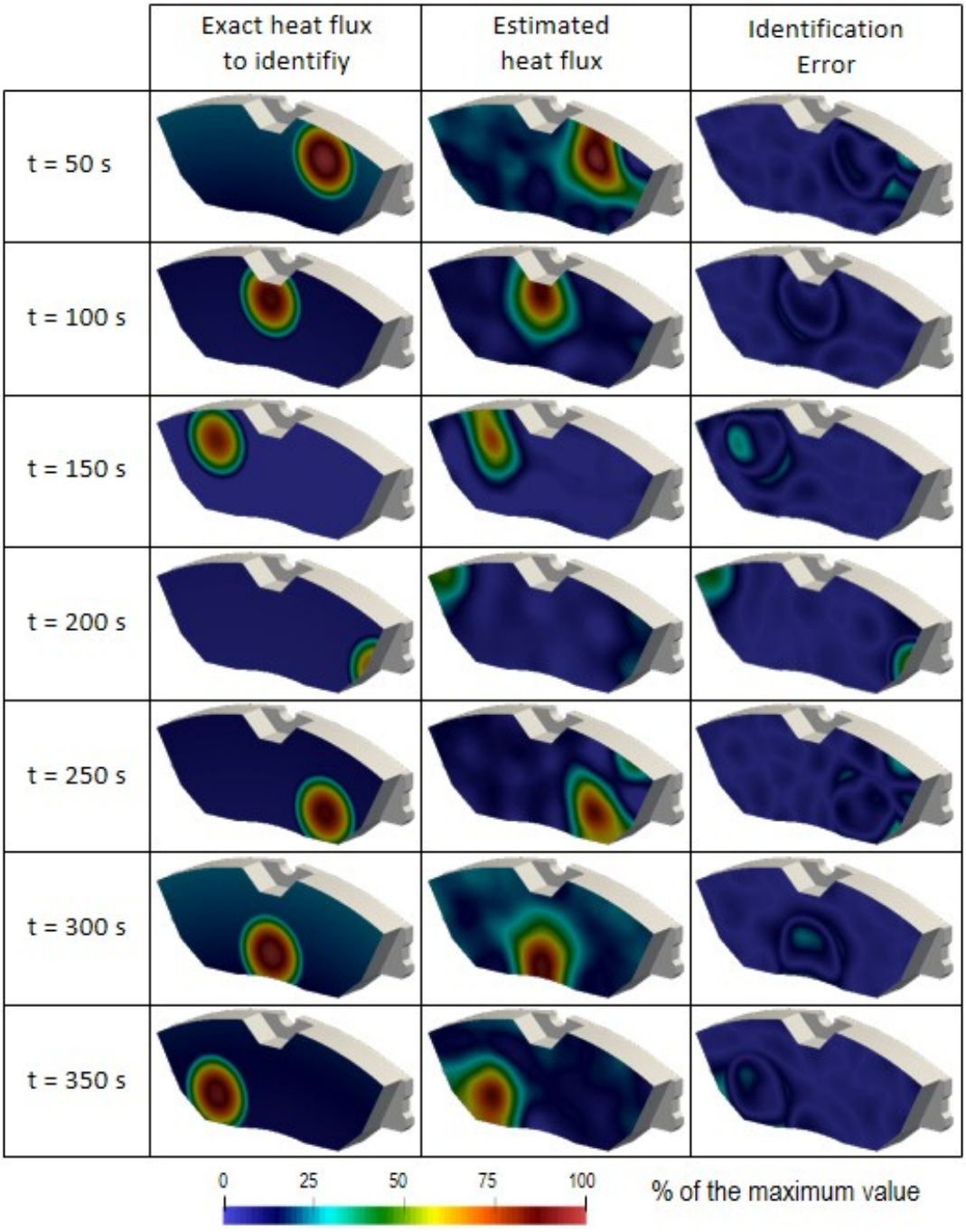

Figure 13: Space-time identification

References

[1] S. Grosjean, F. Joly, K. Vera, A. Neveu, E. Monier-Vinard, Reduction of an electronic card thermal problem by the modal substructuring method, 16th International Hreat Transfer Conference, August 10-15, Beijing, China (2018).

[2] B. Gaume, F. Joly, O. Quéméner, Modal reduction for a problem of heat transfer with radiation in an enclosure, International Journal of Heat and Mass Transfer (2019). doi:https://doi.org/10.1016/j.ijheatmasstransfer.2019.07.039.

[3] A. Fic, R. Bialecki, A. Kassab, Solving transient nonlinear heat conduction problems by proper orthogonal decomposition and the finite-element method, Numerical Heat Transfer, Part B: Fundamentals 48 (2) (2005) 103–124. arXiv:http://dx.doi.org/10.1080/10407790590935920, doi:10.1080/10407790590935920.

[4] X. Zhang, H. Xiang, A fast meshless method based on proper orthogonal decomposition for the transient heat conduction problems, International Journal of Heat and Mass Transfer 84 (2015) 729 – 739. doi:http://dx.doi.org/10.1016/j.ijheatmasstransfer.2015.01.008.

[5] R. Ghosh, Y. Joshi, Error estimation in pod-based dynamic reduced-order thermal modeling of data centers, International Journal of Heat and Mass Transfer 57 (2) (2013) 698 – 707. doi:http://dx.doi.org/10.1016/j.ijheatmasstransfer.2012.10.013.

[6] A. Sempey, C. Inard, C. Ghiaus, C. Allery, Fast simulation of temperature distribution in air conditioned rooms by using proper orthogonal decomposition, Building and Environment 44 (2) (2009) 280 – 289. doi:http://dx.doi.org/10.1016/j.buildenv.2008.03.004.

[7] J. García, J. Cabeza, A. Rodríguez, Two-dimensional non-linear inverse heat conduction problem based on the singular value decomposition, International Journal of Thermal Sciences 48 (6) (2009) 1081 – 1093. doi:http://dx.doi.org/10.1016/j.ijthermalsci.2008.09.002.

[8] A. Rajabpour, F. Kowsary, V. Esfahanian, Reduction of the computational time and noise filtration in the IHCP by using the proper orthogonal decomposition POD method, International Communications in Heat and Mass Transfer 35 (8) (2008) 1024 – 1031. doi:http://dx.doi.org/10.1016/j.icheatmasstransfer.2008.05.004.

[9] H. Park, M. Sung, Sequential solution of a three-dimensional inverse radiation problem, Computer Methods in Applied Mechanics and Engineering 192 (33) (2003) 3689 – 3704. doi:http://dx.doi.org/10.1016/S0045-7825(03)00370-0.

[10] W. Adamczyk, Z. Ostrowski, Retrieving thermal conductivity of the solid sample using reduced order model inverse approach, International Journal of Numerical Methods for Heat & Fluid Flow 27 (3) (2017) 729–739. arXiv:https://doi.org/10.1108/HFF-05-2016-0206, doi:10.1108/HFF-05-2016-0206.

[11] M. Girault, D. Petit., Identification methods in nonlinear heat conduction. Part I: Model Reduction, International Journal of Heat and Mass Transfer 48 (2005) 105–118.

[12] M. Girault, D. Petit, Identification methods in nonlinear heat conduction. Part II: inverse problem using a reduced model, International Journal of Heat and Mass Transfer 48 (1) (2005) 119 – 133. doi:DOI: 10.1016/j.ijheatmasstransfer.2004.06.033.

[13] E. Videcoq, M. Girault, V. Ayel, C. Romestant, Y. Bertin, On-line thermal regulation of a capillary pumped loop via state feedback control using a low order model, Applied Thermal Engineering 108 (2016) 614 – 627. doi:http://dx.doi.org/10.1016/j.applthermaleng.2016.07.071.

[14] M. Girault, E. Videcoq, D. Petit, Estimation of time-varying heat sources through inversion of a low order model built with the modal identification method from in-situ temperature measurements, International Journal of Heat and Mass Transfer 53 (1) (2010) 206 – 219. doi:http://dx.doi.org/10.1016/j.ijheatmasstransfer.2009.09.040.

[15] K. Bouderbala, H. Nouira, E. Videcoq, M. Girault, D. Petit, MIM, FEM and experimental investigations of the thermal drift in an ultra-high precision set-up for dimensional metrology at the nanometre accuracy level, Applied Thermal Engineering 94 (2016) 491 – 504. doi:http://dx.doi.org/10.1016/j.applthermaleng.2015.09.092.

[16] E. Videcoq, M. Girault, A. Piteau, Thermal control via state feedback using a low order model built from experimental data by the modal identification method, International Journal of Heat and Mass Transfer 55 (5) (2012) 1679 – 1694. doi:http://dx.doi.org/10.1016/j.ijheatmasstransfer.2011.11.023.

[17] J. Berger, S. Guernouti, M. Woloszyn, F. Chinesta, Proper generalised decomposition for heat and moisture multizone modelling, Energy and Buildings 105 (2015) 334 – 351. doi:http://dx.doi.org/10.1016/j.enbuild.2015.07.021.

[18] J. Berger, W. Mazuroski, N. Mendes, S. Guernouti, M. Woloszyn, 2d whole-building hygrothermal simulation analysis based on a pgd reduced order model, Energy and Buildings 112 (2016) 49 – 61. doi:http://dx.doi.org/10.1016/j.enbuild.2015.11.023.

[19] J. Berger, N. Mendes, An innovative method for the design of high energy performance building envelopes, Applied Energy 190 (2017) 266 – 277. doi:http://dx.doi.org/10.1016/j.apenergy.2016.12.119.

[20] D. González, F. Masson, F. Poulhaon, A. Leygue, E. Cueto, F. Chinesta, Proper generalized decomposition based dynamic data driven inverse identification, Mathematics and Computers in Simulation 82 (9) (2012) 1677 – 1695. doi:http://dx.doi.org/10.1016/j.matcom.2012.04.001.

[21] C. Lanczos, An iteration method for the solution of the eigenvalue problem of linear differential and integral operators, Journal of Research of the National Bureau of Standards 45 (1950) 255–282. doi:10.6028/jres.045.026.

[22] R. Radke, A matlab implementation of the implicitly restarted arnoldi method for solving large-scale eigenvalues problems, Ph.D. thesis, A thesis submitted in partial fullfillment of the requirements for the degree Master of Arts, Rice University, Houston, Texas (1996).

[23] R. Lehoucq, D. Sorensen, C. Yang, ARPACK Users' Guide: Solution of Large-scale Eigenvalue Problems with Implicitly Restarted Arnoldi Methods, SIAM e-books, Society for Industrial and Applied Mathematics (SIAM, 3600 Market Street, Floor 6, Philadelphia, PA 19104), 1998.

[24] J. Sicard, P. Bacot, A. Neveu, Analyse modale des échanges thermiques dans le bâtiment, International Journal of Heat and Mass Transfer 28 (1) (1985) 111 – 123. doi:http://dx.doi.org/10.1016/0017-9310(85)90013-4.

[25] P. Bacot, A. Neveu, J. Sicard, Analyse modale des phénomènes thermiques en régime variable dans le bâtiment, Revue Générale de Thermique 267 (1984) 189–201.

[26] G. Lefebvre, J. Bransier, A. Neveu, Simulation du comportement thermique d'un local par des méthodes numériques d'ordre réduit, Revue Générale de Thermique 302 (1987) 106–114.

[27] J. Salgon, A. Neveu, Application of modal analysis to modelling of thermal bridges in buildings, Energy and Buildings 10 (2) (1987) 109 – 120. doi:http://dx.doi.org/10.1016/0378-7788(87)90013-2.

[28] A. Neveu, K. El-Khoury, B. Flament, Simulation de la conduction non linéaire en régime variable: décomposition sur les modes de branche, International Journal of Thermal Sciences 38 (4) (1999) 289 – 304. doi:http://dx.doi.org/10.1016/S1290-0729(99)80095-7.

[29] O. Quéméner, A. Neveu, E. Videcoq, A specific reduction method for the branch modal formulation: Application to a highly non-linear configuration, International Journal of Thermal Sciences 46 (9) (2007) 890 – 907. doi:DOI: 10.1016/j.ijthermalsci.2006.11.011.

[30] E. Videcoq, O. Quéméner, W. Nehme, A. Neveu, Real time heat sources identification by a branch eigenmodes reduced model, in: 6th International Conference on Inverse Problems in Engineering, Theory and Practice, Dourdan (France), and in Journal of Physics: Conference Series 135 (freely available on line, paper n 012101), 2008.

[31] E. Videcoq, O. Quéméner, M. Lazard, A. Neveu, Heat source identification and on-line temperature control by a branch eigenmodes reduced model, International Journal of Heat and Mass Transfer 51 (19-20) (2008) 4743 – 4752. doi:DOI: 10.1016/j.ijheatmasstransfer.2008.02.029.

[32] E. Videcoq, M. Lazard, O. Quéméner, A. Neveu, Online temperature prediction using a branch eigenmode reduced model applied to cutting process, Numerical Heat Transfer, Part A: Applications 55 (7) (2009) 683–705. arXiv:http://dx.doi.org/10.1080/10407780902821490, doi:10.1080/10407780902821490.

[33] F. Joly, O. Quéméner, A. Neveu, Modal reduction of an advection-diffusion model using a branch basis, Numerical Heat Transfer, Part B: Fundamentals 53 (5) (2008) 466–485. doi:10.1080/10407790701849550.

[34] O. Quéméner, F. Joly, A. Neveu, On-line heat flux identification from a rotating disk at variable speed, International Journal of Heat and Mass Transfer 53 (7) (2010) 1529 – 1541. doi:http://dx.doi.org/10.1016/j.ijheatmasstransfer.2009.11.032.

[35] P. Laffay, O. Quéméner, A. Neveu, Developing a method for coupling branch modal models, International Journal of Thermal Sciences 48 (6) (2009) 1060 – 1067. doi:http://dx.doi.org/10.1016/j.ijthermalsci.2008.11.002.

[36] P. O. Laffay, O. Quéméner, A. Neveu, B. Elhajjar, The modal substructuring method: An efficient technique for large-size numerical simulations, Numerical Heat Transfer, Part B: Fundamentals 60 (4) (2011) 278–304. doi:10.1080/10407790.2011.609113.

[37] S. Marshall, An approximation method for reducing the order of linear system, control (1966) 642–643.

[38] O. Quéméner, J. Battaglia, A. Neveu, Résolution d'un problème inverse par utilisation d'un modèle réduit modal. application au frottement d'un pion sur un disque en rotation, International Journal of Thermal Sciences 42 (4) (2003) 361 – 378. doi:http://dx.doi.org/10.1016/S1290-0729(02)00037-6.

[39] A. Oulefki, Réduction des modèles thermiques par amalgame modal, Ph.D. thesis, Ecole Nationale de Ponts et Chaussées (1993).

[40] B. Gaume, Réduction d'un problème d'auto-rayonnement par modes de branche : application aux échanges thermiques dans un domaine multi-enceintes, Ph.D. thesis, Paris Saclay (2016).

[41] S. Brou, Modélisation et commande d'un système de cogénération utilisant des énergies renouvelables pour le bâtiment, Ph.D. thesis, Paris Saclay (2015).

[42] O. Quéméner, F. Joly, A. Neveu, The generalized amalgam method for modal reduction, International Journal of Heat and Mass Transfer 55 (4) (2012) 1197 – 1207. doi:http://dx.doi.org/10.1016/j.ijheatmasstransfer.2011.09.043.